A PARAMETER STUDY OF APERTURE-COUPLED CPW-FED STACKED MICROSTRIP ANTENNAS

Steven Mestdagh[(1)], **Guy A.E. Vandenbosch**[(1)]

[(1)] ***K.U.Leuven, dep. ESAT-TELEMIC, Kasteelpark Arenberg 10, B-3001 Heverlee, Belgium***
Tel: +32 16 321150, Fax: +32 16 321986, E-mail: steven.mestdagh@esat.kuleuven.ac.be

ABSTRACT

A parameter study of aperture-coupled stacked patch antennas, fed by coplanar waveguide (CPW) and to be used at millimeter-wave frequencies, is presented. The influence of the most important design parameters was studied. It was found that impedance matching can easily be achieved by tuning the dimensions of the excitation slot and adding an impedance tuning stub. In this way, an antenna element with a –10 dB impedance bandwidth of 36.8 % was designed. This study has led to more insight in the coupling mechanism between the different resonators, allowing a more efficient design of CPW-fed stacked patch antennas.

INTRODUCTION

Aperture coupling is an interesting technique to feed antennas operating at millimeter-wave frequencies (around 30 GHz in this case). At these frequencies microstrip antennas become very small, reducing the suitability of coaxial feeding, as probes are accompanied by soldering points, introducing parasitic inductances. Aperture coupling, however, provides lower parasitic radiation and the centered feed provides higher radiation pattern symmetry [1]. Variation of the aperture dimensions facilitates impedance matching [1]. It is known that the coupling of several resonances leads to a significant increase in bandwidth, which is desired in many applications in the field of telecommunications, e.g. for wireless links with high information capacity. In this paper we wish to provide a systematic parameter study of an aperture-coupled stacked dual patch antenna on glass substrates with an intermediate permittivity ($\varepsilon_r = 6.2$), fed by CPW and thus eliminating the need for a separate feed substrate, which was required to accomodate the feeding microstrip line in [2]. Recently CPW has been used as a worthy alternative to microstrip line feeding and provides several advantages: low dispersion, good characteristic impedance control, easy integration with shunt lumped elements and active devices [3]. The main issue in this study is to investigate the impedance behavior of the structure.

ANTENNA CONFIGURATION

The antenna configuration, which is shown in Fig. 1, consists of a ground plane carrying the CPW terminated in an excitation slot, a substrate, a lower square patch, a second substrate on top of it and an upper square patch. The center conductor of the CPW is connected to the ground plane, which means the slot is short-circuited. The slot is inductively coupled because the impedance locus lies in the inductive region on the Smith chart. This configuration allows easier impedance matching than its counterpart, the capacitively coupled slot, which is open-circuited [4]. Therefore the inductively coupled excitation slot is chosen for an investigation of the stacked patch configuration.
The lower substrate has thickness H_1, relative permittivity $\varepsilon_{r,1}$ and relative permeability $\mu_{r,1}$. The upper substrate has thickness H_2, relative permittivity $\varepsilon_{r,2}$ and relative permeability $\mu_{r,2}$. A MultiChip Module technology with deposited thin films (MCM-D) is used to build some test antennas. This technology focuses on glass substrates ($\varepsilon_{r,1} = \varepsilon_{r,2} = 6.2$ and $\mu_{r,1} = \mu_{r,2} = 1$) for their ease of treatment during the process and for the low material cost. The main interest here was to construct a high bandwidth antenna using these glass substrates, despite the relatively high permittivity. Both substrates are glued together by a thin BenzoCycloButene (BCB) film (with parameters $H_B = 5$ μm, $\varepsilon_{r,B} = 2.7$, $\mu_{r,B} = 1$). Because the BCB layer's thickness is very small compared to the considered wavelengths, its influence is negligible. The lower and upper square patch have dimensions L and U, respectively. The excitation slot has length L_s and width W_s. The patches are centered with respect to each other and the excitation slot is aligned under the center of the patches. The coplanar waveguide has a center conductor width W and a slot width G.

PARAMETER STUDY

In this section a systematic parameter study is performed. The dimensions of the CPW are chosen such that an odd mode characteristic impedance of 50 Ω is obtained: $G = 25$ μm and $W = 100$ μm. Resonant frequencies are defined at maxima

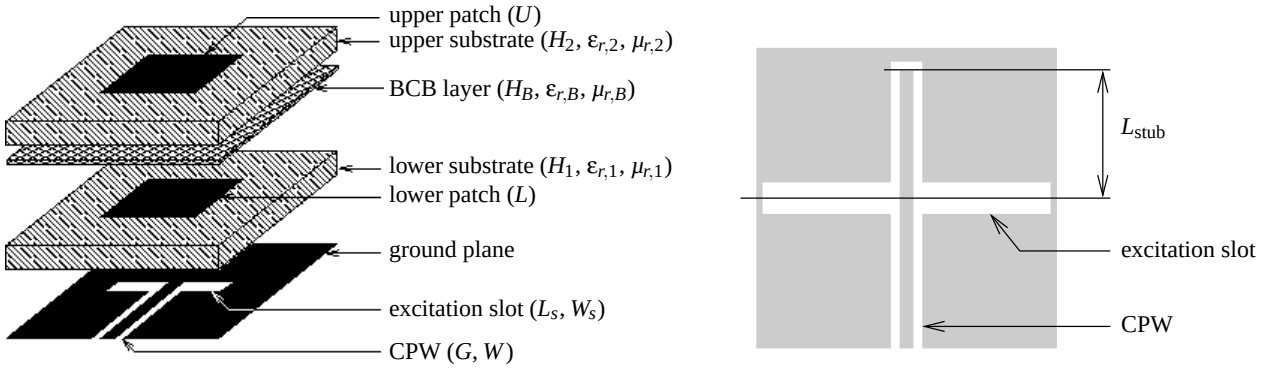

Fig. 1: Stacked patch antenna configuration (left) and impedance tuning stub layout (right)

of the real part of the input impedance $Z_{\text{in}}(f)$. To compensate for the inductive part of the input impedance, caused by the excitation slot, an impedance tuning stub is added, as depicted in Fig. 1 and explained further in this paper.
The two patches and the excitation slot in the ground plane form a resonating structure, which exhibits two coupling effects: one between the slot and the lower patch, another between the patches. The self-resonance of the excitation slot lies above the considered frequency band (20–45 GHz). On the Smith chart the impedance locus contains two loops. The larger the radius of such a loop, the greater the coupling factor. Each physical parameter, except for $\varepsilon_{r,1}$ and $\varepsilon_{r,2}$, will be varied, keeping the other parameters fixed, and its influence will be discussed. Unless mentioned otherwise, the slot width $W_s = 0.1$ mm and the stub length $L_{\text{stub}} = 0.8$ mm. The analysis is based on the solution of integral equations solved in the spectral domain by the method of moments. Agilent Technologies' Momentum is used as a simulation tool. The electric and magnetic surface currents are discretized using rooftop expansion functions defined over the cells in the mesh. For this structure, a mesh of 20 cells per wavelength, combined with edge expansion functions, gives accurate results.

Variation of the Patch Dimensions U and L

In the absence of the upper patch, the impedance locus contains one loop. At the resonant frequency f_1 the input resistance reaches a maximum R_1, where $R_1 = \text{Re}\{Z_{\text{in}}(f_1)\}$. If U becomes comparable to L, a new resonance (f_2,R_2) appears, where $f_2 > f_1$ and $R_2 = \text{Re}\{Z_{\text{in}}(f_2)\}$. The impedance locus starts to form a second loop, as can be seen in Fig 2a. The patches begin to couple to each other. For larger U, the radius of the higher frequency loop increases and the radius of the lower frequency loop decreases a little (see Fig 2b and 2c). The lower patch couples to the excitation slot as well as to the upper patch, so the coupling to the slot is slightly reduced. This result is similar to that in [5].
A variation of L reveals results similar to those mentioned above. If the lower patch is absent, there is again one resonance caused by the upper patch. If a small lower patch is introduced ($L \ll U$), a second resonance is observed at high frequency. It is the slot resonance which transforms to a patch resonance by shifting down in frequency and reducing its bandwidth as L is increased. When $L \approx U$, R_2 decreases until the second resonance disappears. On the Smith charts in Fig. 3 the radius of the higher frequency loop decreases considerably for increasing L. From that point the upper patch is shielded from the excitation slot by the lower patch. For larger values of L ($L \gg U$), the structure behaves as if there were only the lower patch. Correspondingly there is a single resonance (f_1,R_1) and f_1 shifts down for increasing L. To summarize these results, it can be noted that f_1 is determined by U if $U/L \gg 1$ and by L if $U/L \ll 1$. When $U/L \approx 1$, a second resonance is observed. Note that it is not the absolute value of the patches' dimensions that is important, but their sizes relative to one another. This fact is easily confirmed by comparing Fig. 3a to Fig. 2c and Fig. 3c to Fig. 2a.

Variation of the Excitation Slot Dimensions L_s and W_s

The length L_s of the excitation slot is another parameter which has a considerable influence on the resonant frequencies and on the impedance behavior. It is observed that f_1 shifts down and R_1 rises as L_s is increased. If $X_1 = \text{Im}\{Z_{\text{in}}(f_1)\}$, it is observed that $X_1 \sim L_s$, which is a result similar to those in [2], [4] and [6]. Frequency f_2 shifts down for increasing L_s, but this shift is quite small compared to that of f_1. This seems logical since f_2 is mainly determined by U and the upper patch is somewhat shielded from the excitation slot by the lower patch. On the Smith charts in Fig. 4 the main loop becomes larger for increasing L_s. For a certain value of L_s, this loop will touch the circle $r = 1$. Therefore, this parameter can be used for impedance matching, if the inductive component X_1 can be neutralized. The radius of the small loop increases as L_s is increased, reaches a maximum and decreases again for very large L_s. This smaller loop rotates in a clockwise

direction with respect to the main loop as L_s increases.
The parameter W_s has an effect similar to that of L_s. It is observed that f_1 decreases slightly and R_1 as well as X_1 increase almost linearly with increasing W_s. The second resonance is affected much less by a variation of W_s.

Variation of the Substrate Thicknesses H_1 and H_2

The thickness H_1 of the lower substrate affects only the first resonance (f_1,R_1) considerably. As expected, f_1 shifts down as H_1 is increased. The influence of H_1 on the second resonance is small. It is noted that the bandwidth of the first resonance increases as H_1 is increased. On the Smith chart the radius of the lower frequency loop decreases if H_1 is increased. This behavior was expected as the patch is moved further away from the excitation slot, thus reducing the coupling [5].
The thickness H_2 of the upper substrate has a considerable influence on both resonances and on the input impedance. An important consequence of raising H_2 is an increase in bandwidth. Another observation is that f_2 shifts down more than f_1 if H_2 is increased, so the ratio f_2/f_1 is lowered and the two resonant frequencies lie closer to each other, which is also noted in [2]. The impedance curve versus frequency becomes smoother. On the Smith charts in Fig. 5, the radius of the smaller loop in the impedance locus and the coupling between the two patches decrease as H_2 is raised (see also [5]). The loops also shift in the frequency band as explained above.

Design example

A wide-band test antenna was designed around 30 GHz. To achieve impedance matching a tuning stub was added as depicted in Fig. 1. The required stub length L_{stub} is shorter for an electrically open-ended stub than for an electrically short-circuited stub and is approximately $\lambda_1/4$, where $\lambda_1 = \lambda_0/\sqrt{\varepsilon_1}$ and λ_0 is the free space wavelength. This antenna's physical parameters are: $H_1 = 0.3$ mm, $H_2 = 0.7$ mm, $L = 1.4$ mm, $U = 1.425$ mm, $L_s = 1.58$ mm, $W_s = 0.1$ mm. Its main characteristics are: $f_1 = 25.2$ GHz, $f_2 = 33.2$ GHz, $R_1 = R_2 \approx 60\ \Omega$. The –10 dB bandwidth is 10.73 GHz or 36.8 %, while the –15 dB bandwidth is still 9.27 GHz or 31.8 %. The antenna gain in broadside direction is about 3 dB and shows two maxima, which are each located higher in frequency than the input resistance maxima at f_1 and f_2.

CONCLUSIONS

Extensive simulations have led to a better understanding of the mechanism of an aperture-coupled dual stacked patch configuration fed by coplanar waveguide. A detailed parameter study was performed regarding impedance characteristics. The results of this study have been summarized in this paper and are of practical importance to designers of this type of antenna element. This is especially so for the glass substrates employed in MCM-D technology, but the main trends in the results can surely be extended to substrates with different permittivities. Careful inspection of the results of this study has allowed to gain insight in the operation of stacked patch antennas fed by CPW and to design a wide-band antenna with a –10 dB bandwidth of over 30 %.

REFERENCES

[1] L. Giauffret and J.-M. Laheurte, "Theoretical and experimental characterisation of CPW-fed microstrip antennas," *IEE Proceedings Microwaves, Antenna and Propagation*, vol. 143, no. 1, pp. 13–17, February 1996.

[2] F. Croq and D.M. Pozar, "Millimeter-Wave Design of Wide-Band Aperture-Coupled Stacked Microstrip Antennas," *IEEE Transactions on Antennas and Propagation*, vol. 39, no. 12, pp. 1770–1776, December 1991.

[3] E.A. Soliman, S. Brebels, G.A.E. Vandenbosch, and E. Beyne, "Antenna Arrays in MCM-D technology Fed by Coplanar CPW networks," *IEEE Transactions on Microwave Theory and Techniques*, vol. 48, no. 6, pp. 1065–1068, June 2000.

[4] S.-M. Deng, M.-D. Wu, and P. Hsu, "Impedance Characteristics of Microstrip Antennas Excited by Coplanar Waveguide with Inductive or Capacitive Coupling Slots," *IEEE Microwave and Guided Wave Letters*, vol. 5, no. 11, pp. 391–393, November 1995.

[5] S.D. Targonski, R.B. Waterhouse, and D.M. Pozar, "Design of Wide-Band Aperture-Stacked Patch Microstrip Antennas," *IEEE Transactions on Antennas and Propagation*, vol. 46, no. 9, pp. 1245–1251, September 1998.

[6] P.L. Sullivan and D.H. Schaubert, "Analysis of an Aperture-Coupled Microstrip Antenna," *IEEE Transactions on Antennas and Propagation*, vol. 34, no. 8, pp. 977–984, August 1986.

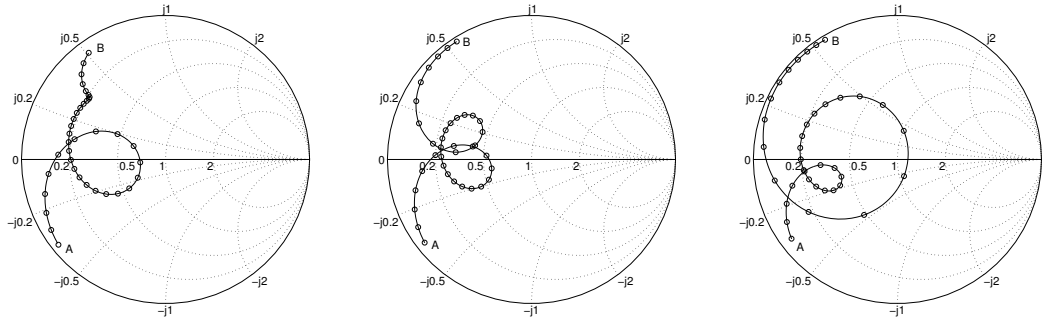

Fig. 2: Impedance loci: (a) $U = 1.2$ mm, (b) $U = 1.35$ mm, (c) $U = 1.5$ mm. Other parameters: $H_1 = 0.3$ mm, $H_2 = 0.5$ mm, $L = 1.4$ mm, $L_s = 1.25$ mm. Frequency range A-B: 24-42 GHz with 0.5 GHz increments.

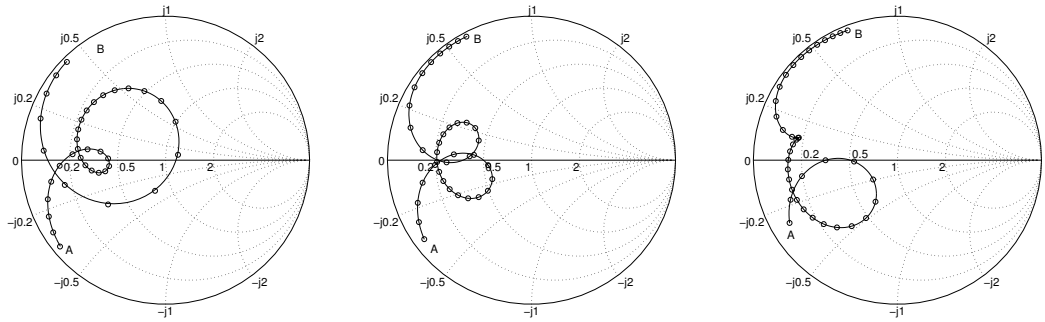

Fig. 3: Impedance loci: (a) $L = 1.3$ mm, (b) $L = 1.45$ mm and (c) $L = 1.6$ mm. Other parameters: $H_1 = 0.3$ mm, $H_2 = 0.5$ mm, $U = 1.4$ mm, $L_s = 1.25$ mm. Frequency range A-B: 24-42 GHz with 0.5 GHz increments.

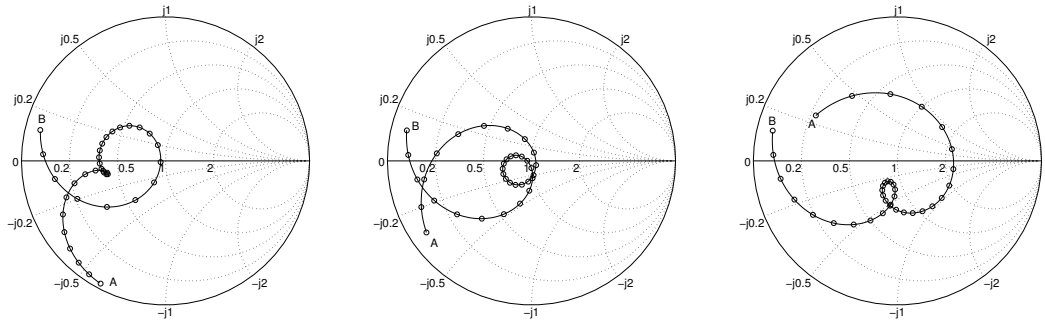

Fig. 4: Impedance loci: (a) $L_s = 1.4$ mm, (b) $L_s = 1.7$ mm and (c) $L_s = 2.0$ mm. Other parameters: $H_1 = 0.3$ mm, $H_2 = 0.7$ mm, $L = 1.4$ mm, $U = 1.4$ mm. Frequency range A-B: 21-38 GHz with 0.5 GHz increments.

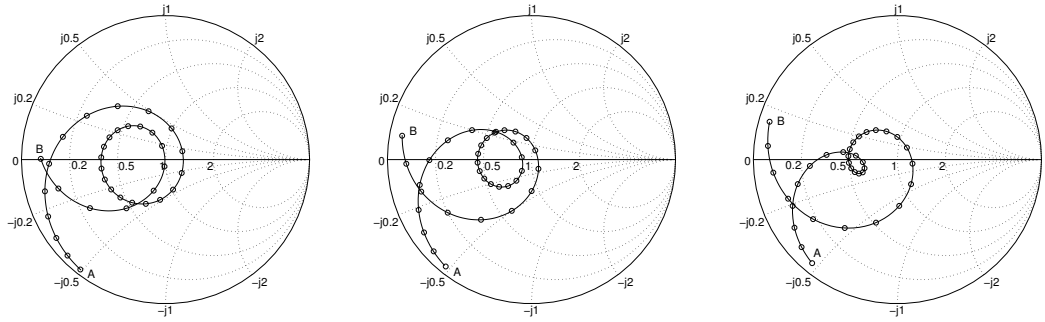

Fig. 5: Impedance loci: (a) $H_2 = 0.5$ mm, (b) $H_2 = 0.6$ mm and (c) $H_2 = 0.7$ mm. Other parameters: $H_1 = 0.3$ mm, $L = 1.4$ mm, $U = 1.45$ mm, $L_s = 1.55$ mm. Frequency range A-B: 21-38 GHz with 0.5 GHz increments.